DEPARTMENT OF COMMERCE
LUTHER H. HODGES, Secretary

WEATHER BUREAU
F. W. REICHELDERFER, Chief

MONTHLY WEATHER REVIEW

JAMES E. CASKEY, JR., Editor

Volume 90, Number 11 | Washington, D.C. | NOVEMBER 1962

SFERICS AMPLITUDE DISTRIBUTION JUMP IDENTIFICATION OF A TORNADO EVENT

DOUGLAS A. KOHL

General Mills Electronics Group, Minneapolis, Minn.

[Manuscript received May 2, 1962; revised August 24, 1962]

ABSTRACT

Changes in the differential pulse height distribution of atmospherics as monitored on 500 kc. sec.$^{-1}$ have been studied on the basis of entire thunderstorm histories. Marked differences in the distribution have been measured associated with different kinds of storms. A storm history unmistakably relating a distribution discontinuity to a tornado event is briefly described.

1. INTRODUCTION

The monitoring of atmospherics at medium frequencies is characterized by extremely high counting rates relative to the typical levels commonly encountered with VLF equipment [1]. The maximum electromagnetic radiative energy associated with pre-discharge sequences, interstroke, and relaxation discharges occurs at medium frequencies [2]. Further, there are a number of intracloud discharges apparently not associated with the "visible" lightning process which are detectable both as sferics and as very small fast step changes in the electric field gradient.

The relationship between severe weather and/or tornado activity and low frequency sferics has been documented [3, 4, 5]. Considerably greater sensitivity in terms of both quantitative and qualitative discrimination of different kinds of thunderstorms is characteristic of sferics monitoring in the frequency domain between 400 and 500 kc. sec.$^{-1}$ [6]. An expanded qualitative interpretation of data gathered at these frequencies has been attempted by examining the sferics amplitude distribution variations. From this study there has emerged a significant relationship between the time derivative variance of the amplitude distributions and severe weather occurrences.

2. TYPICAL AMPLITUDE DISTRIBUTION

The detection process involved a narrow-band antenna and receiver combination centered at 500 kc. sec.$^{-1}$ The detector output was applied to a multi-channel differential pulse amplitude analyzer. The output of each channel was in the form of average count rate. These data were recorded during the entire lifetime of a storm.

The mean distribution derived from 20 different storms closely approximates an exponential form:

$$S(h)=Ne^{-\alpha h}$$

where $S(h)$ is the count rate distribution function; N is the count rate at the limit of detectability [1]; α is a constant of proportionality; and h is the pulse amplitude. The interpretation of this distribution is that there are a large number of small pulses and a very few large pulses in any given sample period. Further, there is little change in the distribution due to propagation distance variables.

A three-dimensional model photographed in figure 1 is representative of the typical distribution form. The bottom dimension of the figure (abscissa) is the pulse amplitude increasing to the right. The vertical dimension

[1] The limit of detectability refers to that defined by the sensitivity of the "finitely wide" lowest counting window of the pulse analyzer.

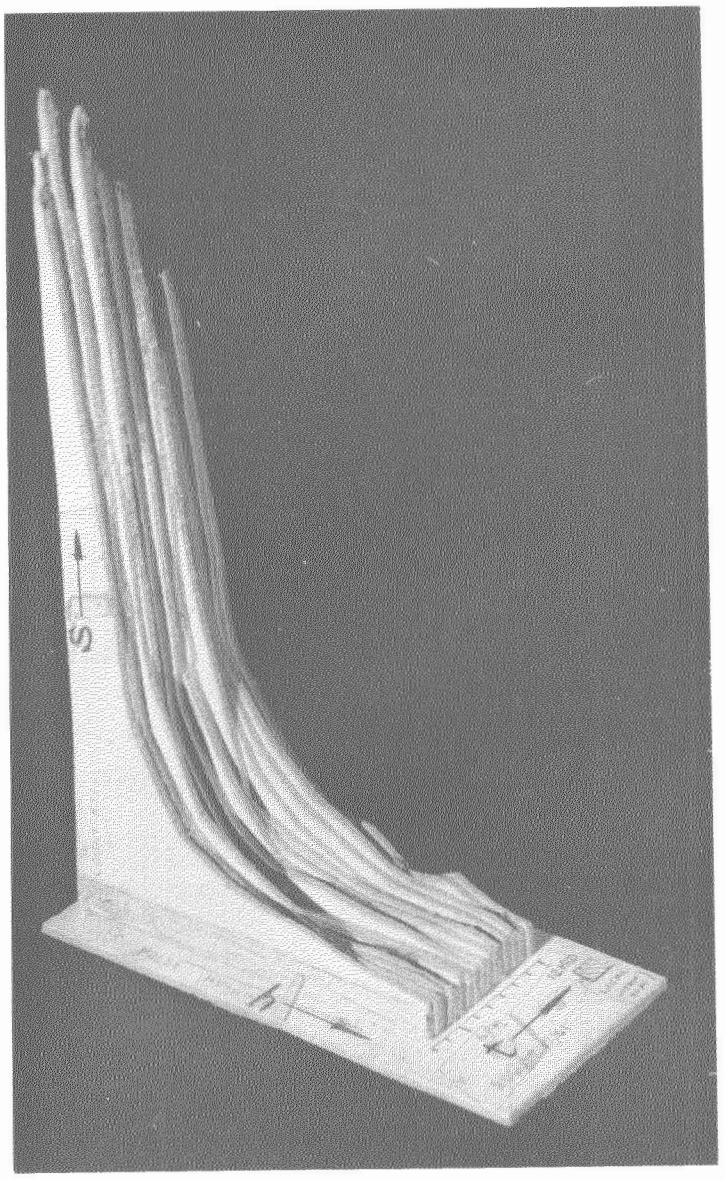

FIGURE 1.—500 kc. sec.$^{-1}$ sferics amplitude distribution history of a thunderstorm (low variability). S = count rate; h = pulse amplitude; t = time.

(ordinate) is the count rate distribution increasing from zero at the base. Each distribution profile was constructed from continuous data sampled at 30-min. intervals so that elapsed time provides the third dimension of the model, increasing in the sense away from the viewer. This is the amplitude distribution history of a single thunderstorm from beginning to end.

Each profile of the model is quite similar to all others, and thus, the surface formed tends to be uniform in the time dimension. The concept of the time derivative of this surface is of importance. By sampling in time and weighting each pulse amplitude channel variance into a composite value according to the coefficients of variation, the total variance of this surface is 0.04. The total variance σ_T^2 is given by

$$\sigma_T^2=\overline{S}^2\left[\left(\frac{\sigma_1}{\overline{S}_1}\right)^2+\left(\frac{\sigma_2}{\overline{S}_2}\right)^2+\ldots+\left(\frac{\sigma_n}{\overline{S}_n}\right)^2\right]$$

where $\sigma_1, \sigma_2, \ldots \sigma_n$ are standard deviations of the channel or derivatives; $\overline{S}_1, \overline{S}_2, \ldots \overline{S}_n$ are the mean channel values; $\overline{S}$ is the mean channel level of all storms measured.

3. EXTENDED STORM HISTORY

The distribution histories of several single thunderstorms in the southern Minnesota region including the two days preceding the tornado event on August 4, 1961 are shown in a single model in the photograph in figure 2. The viewing angle of the model is from above so that elapsed time increases from left to right, increasing pulse height from back to front downward, and the count rate distribution upward and toward the observer. A mirror reflection of the image of the model from a more nearly horizontal perspective permits examination of the absolute sferics count rate profile part of the model.

The absolute count rate is related to the total amount of sferics activity within the storm. The solar thermodynamic diurnal effect on thunderstorm activity is clearly evident in this record. The sferics count rate became zero [2] at mid-day on August 3 and during the aftermidnight period. The different periods of activity were associated with newly formed storms unrelated to previous cloud formations. The presence of a secondary maximum in the form of a hump or continuous "foothill" common to all distribution profiles is of incidental interest, because it appears in each of the thunderstorms during the period. The lighting angle in the photograph was chosen to show this feature.

During the 3 days preceding the tornado, the lower air circulation from the southwest carried humidity into the entire Northern Great Plains. Evidence of the humidity concentration is in the form of the late afternoon air mass thunderstorms as appear in figure 2. During this period, however, a well-defined cold front advanced from the Yukon into Minnesota at a sustained speed of 23 m.p.h.

On August 4, a low pressure trough over eastern Minnesota was in evidence extending ahead of and in the direction of the frontal advance. A well-defined zone of maximum wind extending from 500 to 200 mb. contained winds which intersected this trough at nearly right angles flowing in a northeastward direction. Thunderstorm activity was confined to the vicinity slightly in advance of the front and along the western side of the trough. The front was still definable on the following day well into northern Illinois.

4. AUSTIN, MINN. TORNADO

The tornado occurred in Austin, which is located 104 mi. south of the detection station (near Minneapolis). The tornado was reported suspended beneath a low, dense,

[2] At this frequency and with detector sensitivity employed, signals originating more than 200 mi. distant are not detected, so that in fair weather the count rate is actually zero

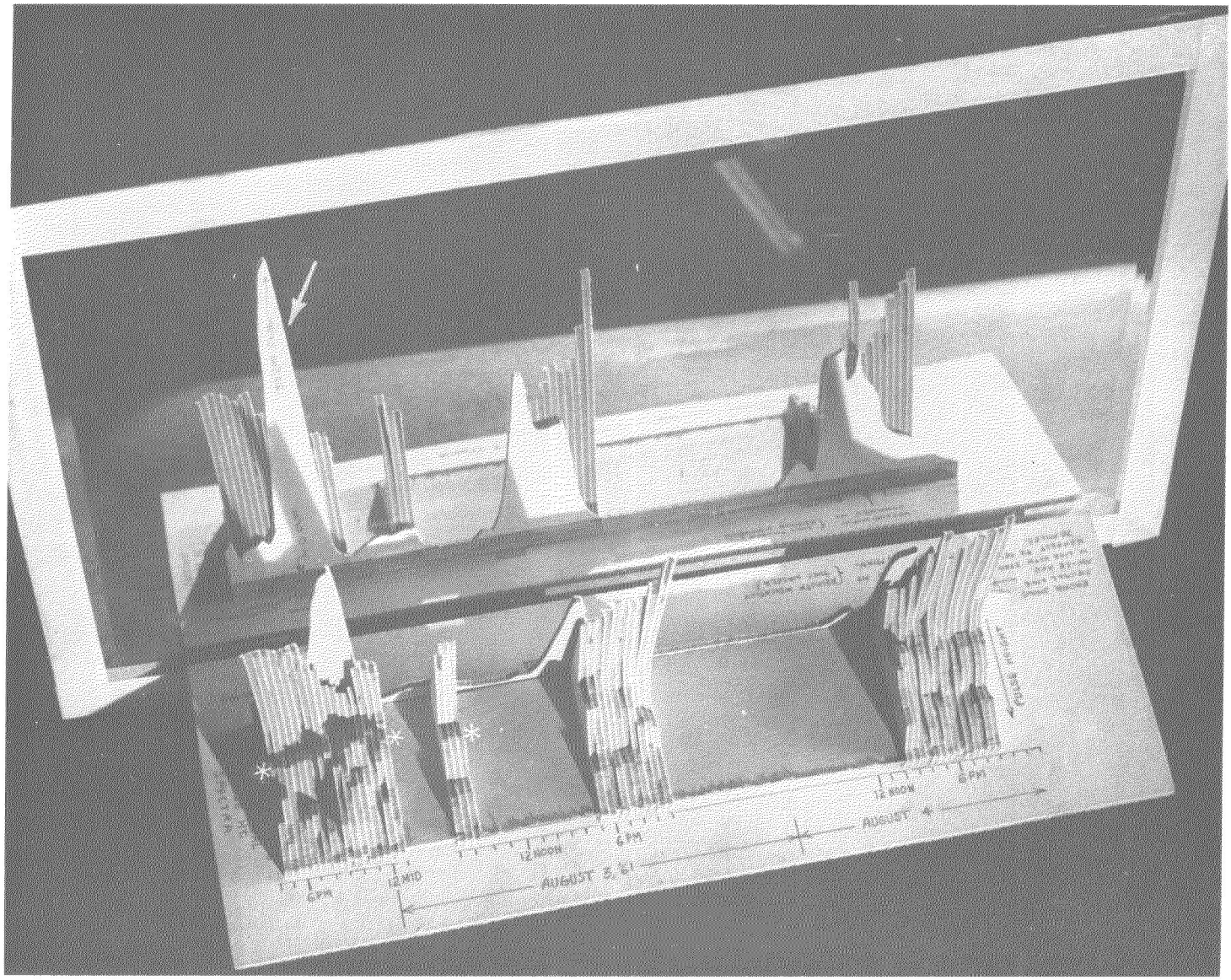

FIGURE 2.—Extended storm history of sferics amplitude distribution, August 2–4, 1961. Arrow points to absolute count rate. Asterisks denote secondary maximum.

swirling cloud with a definite rotational pattern in a horizontal plane. It was associatad with the leading edge of an isolated thunderstorm traveling in a southeasterly direction; however, the destruction path through the city was produced by the tornado funnel moving from SW to NE. Hail and rain occurred north of the contact line. Wind damage along 24 city blocks and eyewitness accounts of many observers have permitted an accurate documentation of the tornado to be made [7].

The first sighting of the tornado funnel was at 1640 CST. The last verification was about 10 min. later to the east of the town. One and a quarter hours later the surface manifestation of the front suddenly passed through the city bringing strong winds and an abrupt drop in temperature.

The map in figure 3 depicts the time sequence of thunderstorm progression, as defined by weather radar,[3] in the area prior to the tornado event. Although radar echoes were broadly distributed during this period, only those returns are shown which were identified by sferics as thunderstorms. Also shown is the position of the front at noon and at 1800 CST.

The tornado was apparently associated with the thunderstorm complex which was already 3½ hr. old at the time of the event. It is of note that this storm did not attain appreciable lateral or vertical development.[4] The thunderstorm which passed through Rochester indicated a very rapid increase in sferics from 1500 to 1600

[3] Bendix WTR-1C (C-band) and Collins WP101 (Airborne), Minneapolis; WSR-57 Des Moines.

[4] Analysis of USWB WSR-57 radar data from Des Moines, Iowa (150 mi. from Austin, Minn.) failed to indicate this storm until 1900 CST, even though the line-of-sight cut-off altitude is only 15,000 ft.

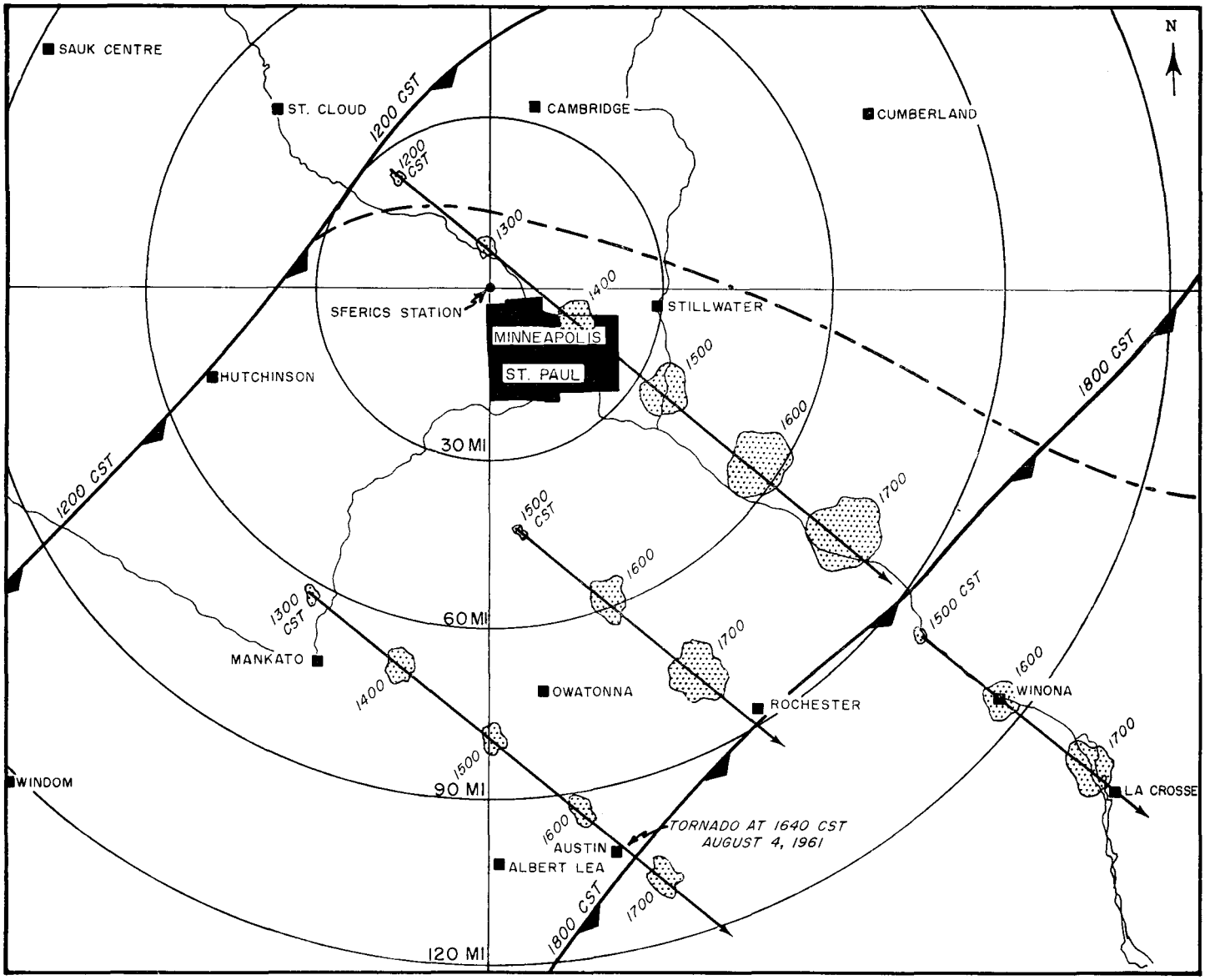

FIGURE 3.—Sferics-radar map of thunderstorm progression, August 4, 1961.

CST and produced hail by 1700 CST. Aside from the tornado at Austin and the hail damage north of Rochester, no other reports of severe weather were received during the passage of the front into Iowa and Illinois.

An enlargement of the August 4 portion of the model in figure 4 shows a simultaneous occurrence of a discontinuity in the amplitude distribution surface and a "sharp" peak or maximum in the total sferics count rate, obtained from the storm which passed through Austin. The abrupt change in the direction is visually most evident in the lower amplitude channels (tallest) as two prominent profiles extending above the adjacent ones. The extent of the variation is emphasized by the shadow angle cast on the model in the foreground. The discontinuity is apparent in the reflected image as well, and, also the time relationship between the sudden peak in absolute count rate and the discontinuity may be visualized. Both occurred at 1632 CST.

The surface created by the distribution profiles actually shows a fairly smooth transition during the portion of the model shown in figure 4. The total variance of the surface, computed as before, is 0.56. This large value is, however, due to tilt of the surface or surface gradient components sustained along the time dimension which exist at nearly every pulse amplitude level rather than random surface irregularities.

This situation is graphically presented in the single channel data shown for the same period in figure 5. The curve in figure 5A represents the count rate variation in channel 1, the lowest amplitude sferics. The mean count rate, $\overline{S}_1$, and the standard deviation limits are indicated.

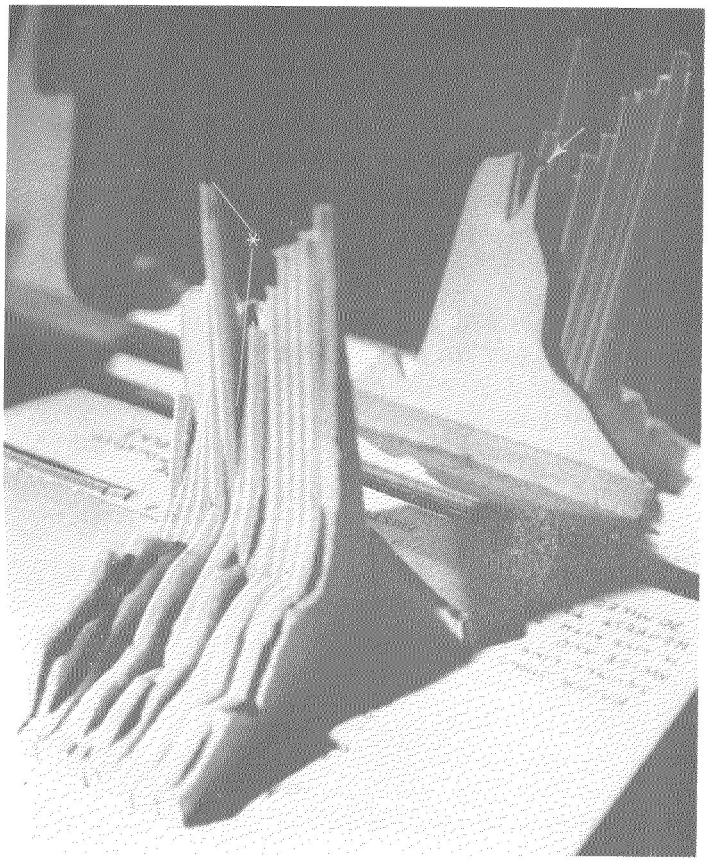

FIGURE 4.—Sferics amplitude distribution history, August 4, 1961. Lines extending from asterisk show the amplitude distribution discontinuity and arrow head points to the concurrent absolute count rate peak.

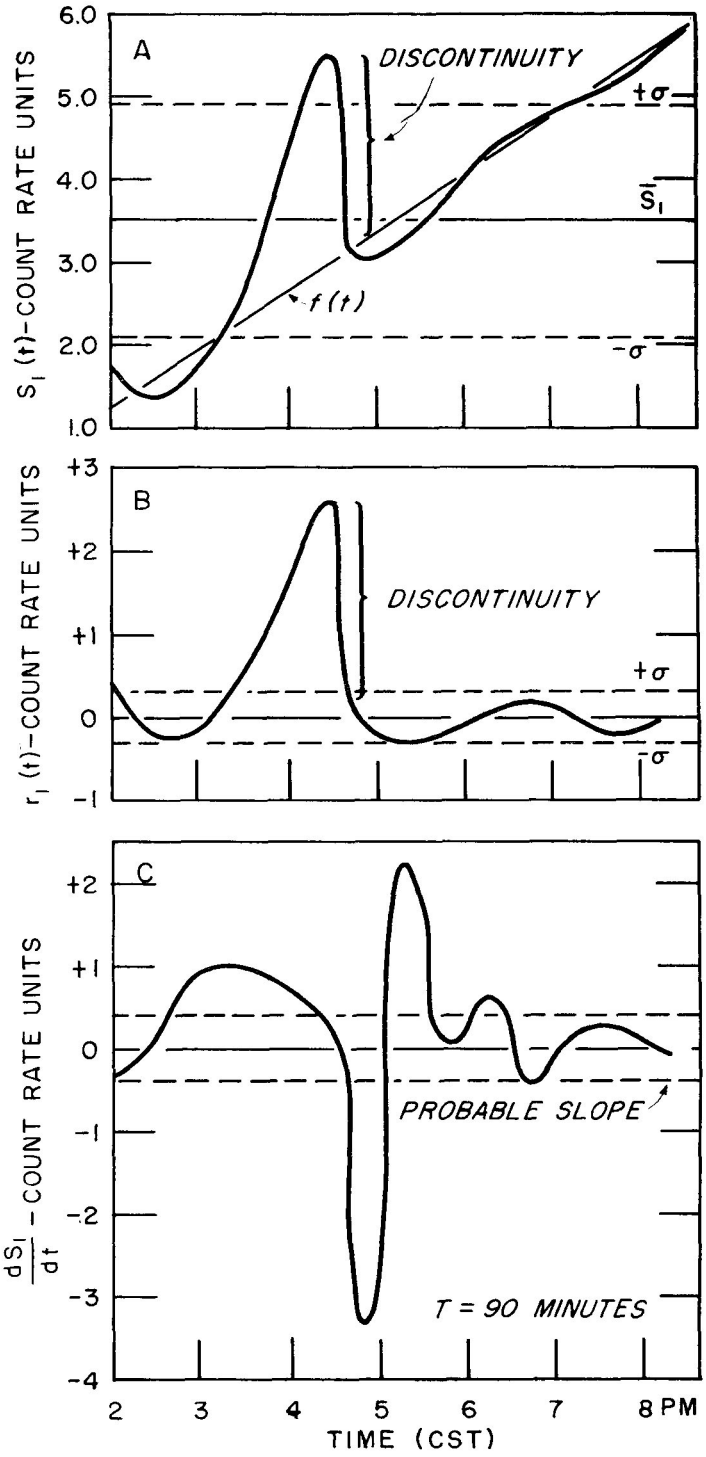

FIGURE 5.—Time distribution of differential pulse height analyzer data, channel 1, August 4, 1961. (A) Count rate variation (channel level). (B) Residuals of channel level from linear approximation (residual variation). (C) Time derivative of channel level (differential variation, 90-min. time constant).

When the instantaneous time derivative of the curve is examined, the slope preceding the abrupt change in slope is 4.4 times greater than the constant gradient of $f(t)$, a linear approximation of the trend. The slope discontinuities in all channels vary in magnitude and sign so that the composite variance derived from various channel levels, each normalized to their mean respective slopes, provides the basis by which to test statistically the significance of individual channel variations relative to the variability of all channels for the entire period.

The channel 1 record happens to contain a nearly linear time function which conveniently illustrates the normalization for a single channel. The residuals of the instantaneous channel level from the linear approximation, $f(t)$, are shown in figure 5B. The composite variance, computed with the residuals from all the channel regression lines $[f(t)]$ within the surface, is 0.06. The maximum deviation represented by the discontinuity of the channel 1 record is 2.2 count-rate units, which exceeds the normalized composite standard deviation limits of the surface (shown on the graph) by 9 times.

The relationship between the statistical description and a continuous time derivative of the storm history is dependent upon sampling frequency, in the former, and the time constant, in the latter. The presence of a linear time trend in all channels of the subject data is indicated by the decrease in composite variance from 0.56 to 0.06

when the individual channel trends were derived. Also, for values of derivative time-constants greater than 10 min. the discontinuity in all channels attains greatest significance with a time constant of nearly 90 min.

On this basis for the channel 1 example, the derivative of the slope discontinuity exceeds by 8.6 times the probable value of the derivative during the entire 3-day period [5] (see fig. 5C).

5. CONCLUSIONS

The use of sampling and conventional statistical analysis is efficient in the evaluation of the general three-dimensional history of sferics amplitude distributions. In the broader program alluded to, which is concerned with thunderstorm evolution, the changes in analyzer channel levels as well as rates of change are possible predictor parameters related to the thermodynamic energy transport process. The tornado event described in this paper differs from all other severe weather dynamical changes observed in a series of 20 storms. The duration of the sustained amplitude distribution distortion buildup and the magnitude of the distribution jump exceed those with other correlations.

It was demonstrated that in this instance of a tornado event, a simple differential measurement with a time constant of 90 min. is the equivalent of the statistical evaluation, and, hence, suggests the basis for instrumentation specifically designed to monitor for distribution distortions of this kind. The Austin tornado may not have been typical inasmuch as it was not part of an extensive severe weather system and perhaps explains the excellent statistical discrimination in which the event record exceeded 8 times the standard deviation.

Although in these data, the beginning of the distribution distortion occurred 105 min. prior to the tornado, it did not exceed three times the standard deviation until 45 min. before. Some similar advance warnings with VLF sferics have been documented by the Air Weather Service [8].

Not enough data have been evaluated at 500 kc. sec.$^{-1}$ to permit anything other than a few generalizations to be made at this time. The unmistakable sudden increase in total sferics count rate, as well as the shift in amplitude distribution toward a much larger proportion of small sferics, appear to be compatible with Gunn's [9] electric field measurement data near a tornado in which the number of field "steps" greatly increased while the magnitude of the change became progressively smaller as the tornado was spawned. However, Gunn's detecting and recording means were both spatially integrated and so restricted in bandwidth that only the trend is evident.

[5] The probable value of slope was derived from the prior and unrelated thunderstorm records as well as the one associated with the tornado event.

Jones [4] has reported visual observations of lightning associated with tornadoes in which there were few cloud-to-ground strokes. A storm developing into this characteristic would probably show a change in the amplitude distribution of sferics; however, a shift of the distribution toward smaller amplitudes simultaneously with a rapid increase in absolute sferics count rate occurs in many rapidly growing thunderstorms [6]. Further, neither the absolute level nor the change in sferics count rate associated with the tornado event exceeds the probable levels obtained from all the data, and to infer tornado warning from count rate alone is dubious.

Speculation concerning the energy source(s) of a tornado includes the possibility of the thermal energy concentration by means of frequent lightning discharges [10]. The tornado vortex, as a distinct partition of the total kinetic energy with the storm, is of limited duration and in the data presented in this paper an indication of great change in the character of the lightning is in evidence. Whether or not the total electrical energy dissipated changes during the tornado has yet to be established.

ACKNOWLEDGMENT

Appreciation is extended to Mr. Denis Dartt who performed a thorough meteorological analysis of available weather data to furnish background information for this paper.

REFERENCES

1. D. A. Kohl, "Short Term Weather Forecasting Using Atmospheric Electrical Phenomena," (Amateur Scientist), *Scientific American*, vol. 200, No. 3, Mar. 1959, p. 155.
2. D. J. Malan, "Radiation from Lightning Discharges and Its Relation to the Discharge Process," *Proceedings of the 2d Conference on Atmospheric Electricity, Portsmouth, N.H., May 20–23, 1958*, Pergamon Press, New York 1958, pp. 557–563.
3. U.S. Air Weather Service, 4th Weather Group, "Project Tornado-Sferics, 1960 Phase," Final Report, (ASTIA AD 254-827) 1961, (see p. 16).
4. H. L. Jones, "The Identification of Lightning Discharges by Sferic Characteristics," *Proceedings of the 2d Conference on Atmospheric Electricity, Portsmouth, N.H., May 20–23, 1958*, Pergamon Press, New York, 1958, pp. 543–556.
5. H. L. Jones and R. D. Kelly, "Research on Tornado Identification: Compendium for Period 1 January 1952 to 31 December 1956," Contract DA-36-039-Sc64436, Oklahoma Agricultural and Mechanical College, 1957.
6. D. A. Kohl, 500 kc. Sferics Amplitude Distribution Measurements of Thunderstorms. (Unpublished data.)
7. *Austin Daily Herald*, vol. 139, No. 30, Aug. 5, 1961, Austin, Minn.
8. U.S. Air Weather Service, "Project Tornado-Sferics," Final Report, 1957. (ASTIA AD 218-741)
9. R. Gunn, "Electric Field Intensity at the Ground Under Active Thunderstorms and Tornadoes," *Journal of Meteorology*, vol. 13, No. 3, June 1956, pp. 269–273.
10. B. Vonnegut, "Electrical Theory of Tornadoes," *Journal of Geophysical Research*, vol. 65, No. 1, Jan. 1960, pp. 203–211.